Supplementary Material for

Non-Covalent Interactions and their Impact on the Complexation Thermodynamics of Noble Gases with Methanol

Lúcio R. Vieira,[‡] Sandro F. de Brito,[‡] Mateus R. Barbosa,[‡] Thiago O. Lopes,[‡] Daniel F. Scalabrini Machado,[‡,*] and Heibbe C. B. de Oliveira[†,*]

[‡]Laboratório de Modelagem de Sistemas Complexos (LMSC), Instituto de Química. Universidade de Brasília. Brasília. Brazil.

[†]Laboratório de Estrutura Eletrônica e Dinâmica Molecular (LEEDMOL), Instituto de Química. Universidade Federal de Goiás. Goiânia. Brazil.

*E-mail: heibbe@ufg.br; daniel.scalabrini@unb.br

Summary

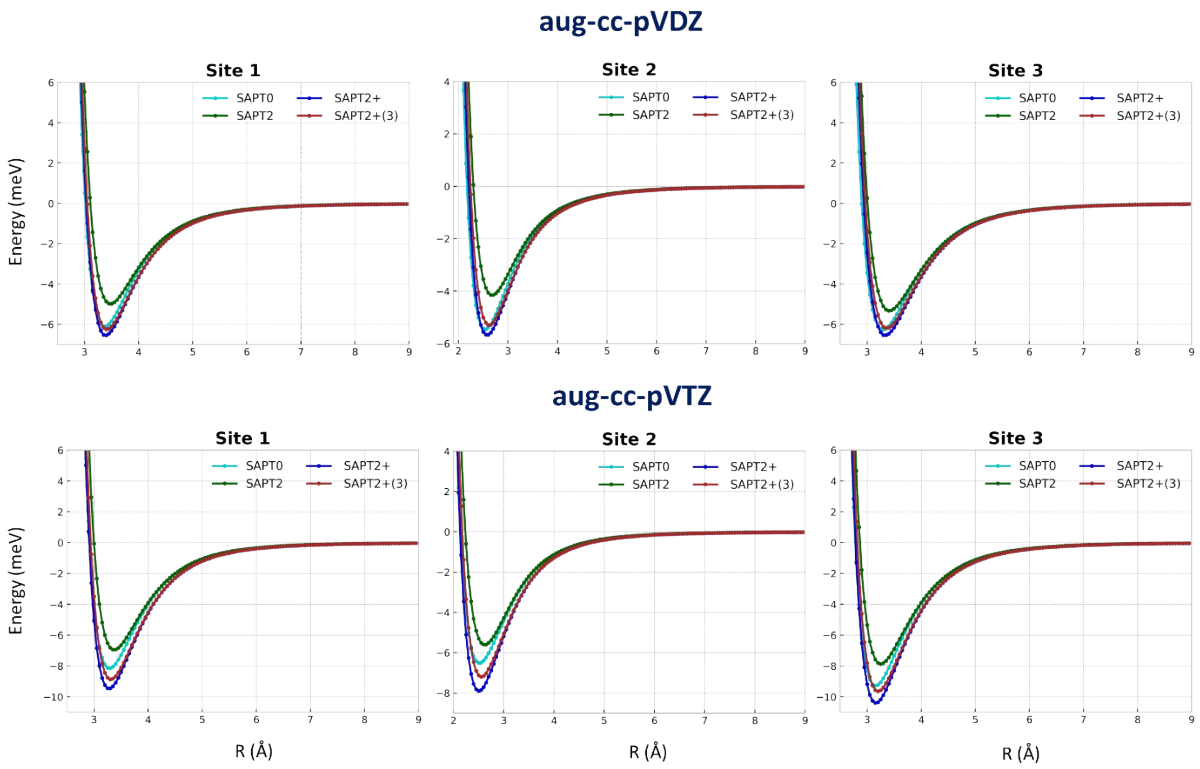

Figure S1. Basis set and SAPT perturbation order effects on the potential energy curves for the Ne-CH_3OH dimers at different interaction sites.

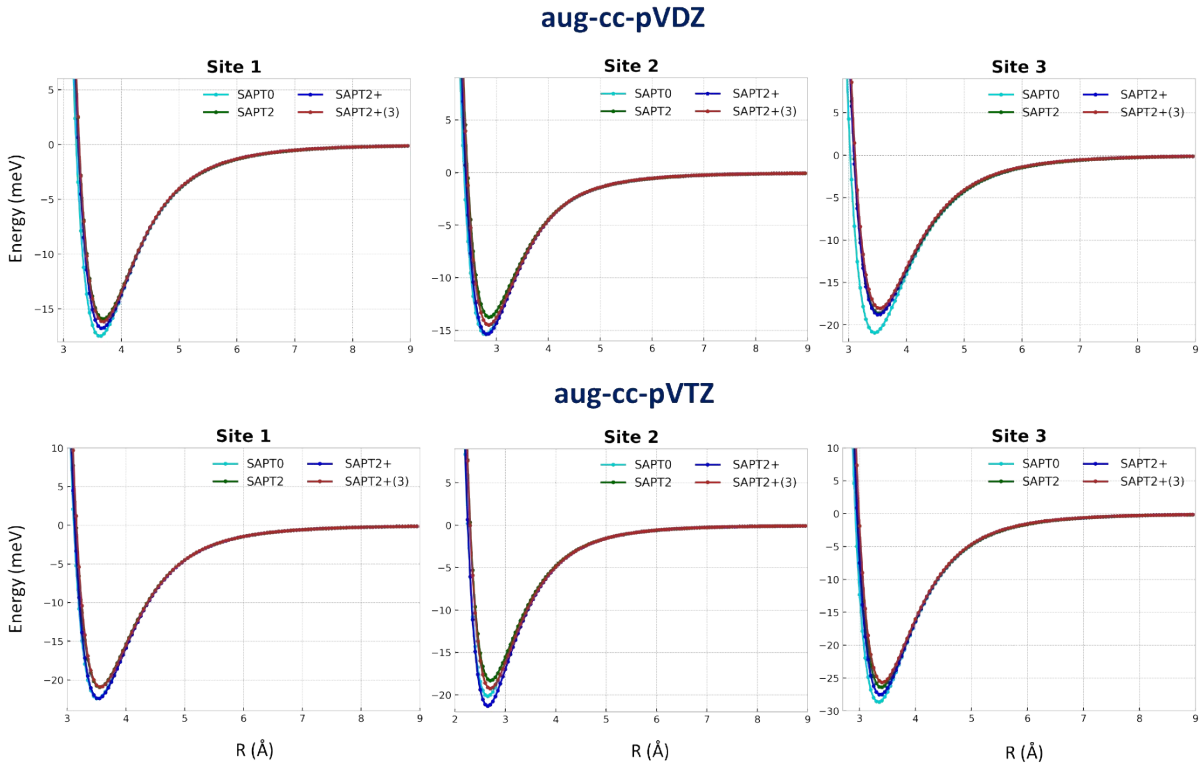

Figure S2. Basis set and SAPT perturbation order effects on the potential energy curves for the Ar-CH_3OH dimers at different interaction sites.

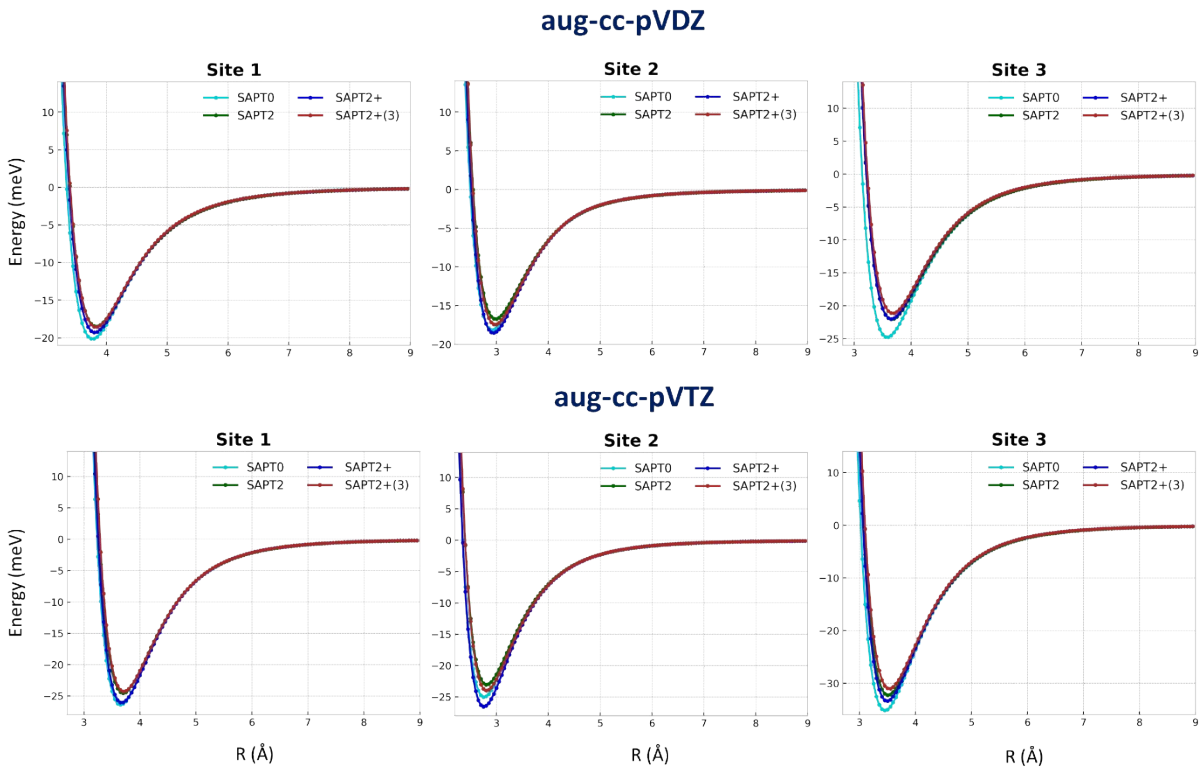

Figure S3. Basis set and SAPT perturbation order effects on the potential energy curves for the Kr-CH_3OH dimers at different interaction sites.

Table S1. Energy decomposition of the intermolecular energies at the equilibrium length R_e for the three interaction sites of Ng-CH_3OH dimers calculated at the SAPT2/aug-cc-pVTZ level of theory for the He and Ne cases; SAPT2/aug-cc-pVDZ for the Ar case and SAPT2+(3)/aug-cc-pVTZ for the Kr case. All energies in meV.

Dimer		E_{lst}	E_{exch}	E_{ind}	E_{disp}	Total
$He-CH_3OH$	Site 1	-1.3573	6.343316	-0.47365	-8.35751	-3.84516
	Site 2	-0.5641	3.28694	-0.94125	-4.23239	-2.4508
	Site 3	-1.10963	5.188201	-0.91114	-7.22365	-4.05622
$Ne-CH_3OH$	Site 1	-3.00423	9.963405	-0.42694	-13.4701	-6.93783
	Site 2	-2.51499	8.066402	-2.03525	-9.11444	-5.59827
	Site 3	-3.42651	11.33454	-1.55427	-14.2176	-7.86379
$Ar-CH_3OH$	Site 1	-6.17318	19.21294	-1.50692	-27.4328	-15.8999
	Site 2	-5.06007	19.4416	-6.30522	-21.8108	-13.7345
	Site 3	-8.2771	25.84336	-4.67862	-31.4816	-18.5939
$Kr-CH_3OH$	Site 1	-7.76375	23.08729	-1.72725	-32.1424	-18.5461
	Site 2	-5.68371	26.15502	-9.146	-28.7355	-17.4101
	Site 3	-9.30291	30.92135	-6.52924	-36.1985	-21.1092

Table S2. Fitted parameters of the Ryd6 and ILJ analytical forms for the He-CH_3OH dimer. Theoretical points calculated at the SAPT2/aug-cc-pVTZ level of theory. Values in parenthesis is relative to the ILJ function.

Parameter	Site 1	Site 2	Site 3
c_1	2.019	2.046	2.858
c_2	-1.348	-1.062	1.169
c_3	1.215	1.074	0.563
c_4	-0.403	-0.348	-3.58×10^{-2}
c_5	7.65×10^{-2}	7.84×10^{-2}	0.485
c_6	-8.99×10^{-4}	-8.29×10^{-6}	3.44×10^{-3}
R_e (Å)	3.25	2.60	3.20
$D_e\,(meV)$	3.88	2.45	4.05
β	7.93	3.81	6.19
χ^2	9×10^{-7} (5×10^{-4})	1×10^{-6} (5×10^{-3})	1×10^{-6} (5×10^{-3})

Table S3. Fitted parameters of the Ryd6 and ILJ analytical forms for the Ne-CH_3OH dimer. Theoretical points calculated at the SAPT2/aug-cc-pVTZ level of theory. Values in parenthesis is relative to the ILJ function.

Parameter	Site 1	Site 2	Site 3
c_1	3.264	1.801	1.973
c_2	1.663	-1.772	-1.202
c_3	2.445	1.714	1.069
c_4	1.887	-0.882	-0.334
c_5	-2.227	0.243	0.065
c_6	1.126	-0.023	-9.37×10^{-7}
R_e (Å)	3.35	2.60	3.25
$D_e\,(meV)$	6.94	5.60	7.86
β	9.50	4.32	7.26
χ^2	1.6×10^{-3} (1×10^{-2})	1.6×10^{-3} (2.2 $\times 10^{-2}$)	1.7×10^{-5} (1.7 $\times 10^{-5}$)

Table S4. Fitted parameters of the Ryd6 and ILJ analytical forms for the Ar-CH_3OH dimer. Theoretical points calculated at the SAPT2/aug-cc-pVDZ level of theory. Values in parenthesis is relative to the ILJ function.

Parameter	Site 1	Site 2	Site 3
c_1	2.894	2.696	2.982
c_2	1.509	0.782	2.041
c_3	0.378	0.967	0.494
c_4	-0.019	0.668	-0.093
c_5	0.648	-0.632	0.909
c_6	1.72×10^{-4}	0.266	1.83×10^{-3}
R_e (Å)	3.70	2.85	3.55
$D_e\,(meV)$	15.90	13.73	18.60
β	7.64	4.15	5.91
χ^2	8×10^{-3} (2.6×10^{-2})	1.4×10^{-4} (2.6	2×10^{-2} (5×10^{-2})

	$\times 10^{-2}$)

Table S5. Fitted parameters of the Ryd6 and ILJ analytical forms for the Kr-CH_3OH dimer. Theoretical points calculated at the SAPT2+(3)/aug-cc-pVDZ level of theory. Values in parenthesis is relative to the ILJ function.

Parameter	Site 1	Site 2	Site 3
c_1	2.694	2.569	2.900
c_2	0.863	0.364	1.789
c_3	0.885	0.658	0.432
c_4	0.618	0.580	-0.016
c_5	-0.501	-0.384	0.654
c_6	0.224	0.146	1.7×10^{-3}
R_e (Å)	3.85	2.95	3.70
$D_e\,(meV)$	18.54	17.41	21.11
β	8.25	3.25	5.85
χ^2	5×10^{-3} (2.2×10^{-2})	3×10^{-3} (0.21)	3.6×10^{-2} (8×10^{-2})

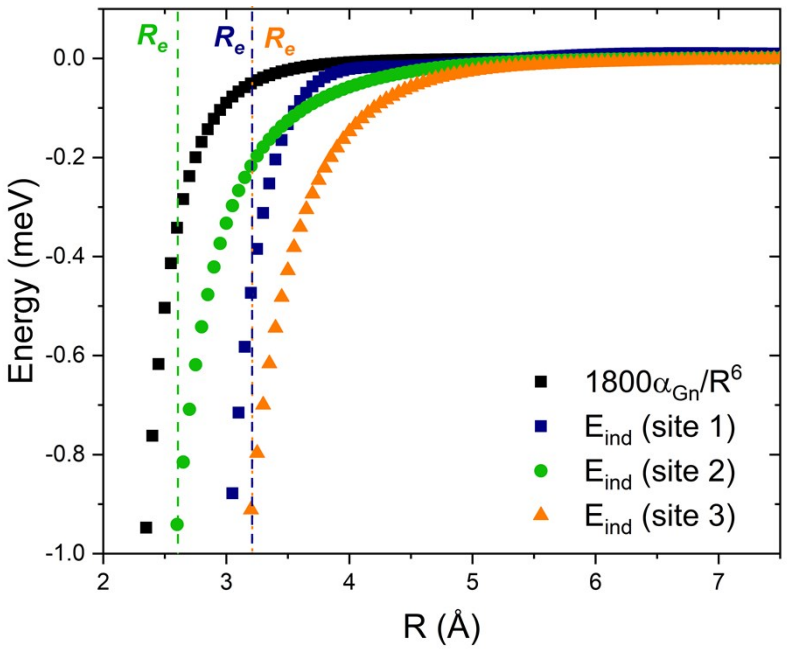

Figure S4. Comparison of induction energies E_{ind} between the semi-empirical formulation based on Debye's formula and the theory calculated at the SAPT2/aug-cc-pVTZ level for the He-CH_3OH dimer. Vertical dashed lines indicate the equilibrium distance of the interacting dimer at different sites on the methanol molecule. The static linear polarizability of He-atom was set to $\alpha_0 = 0.204$ Å^3. Debye's formula for the permanent dipole-induced dipole interaction is given by $E_{ind} = E_{Debye}(R) = -\mu_{CH_3OH}{}^2 \alpha_{Gn} / (4\pi\varepsilon_0)^2 R^6$, with μ_{CH_3OH} standing for the dipole moment of methanol. The numeric coefficient is obtained when meV· Å^3 units are used.

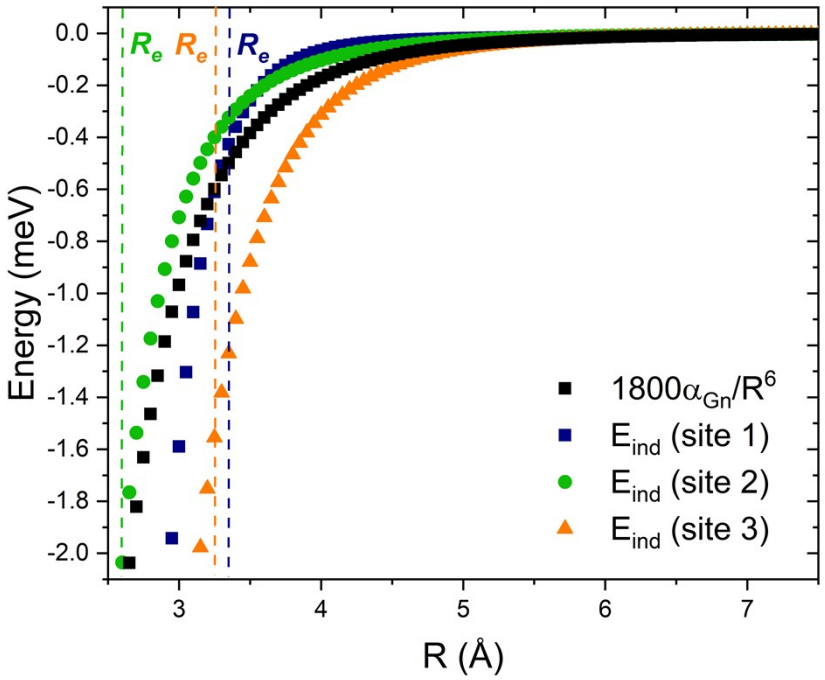

Figure S5. Comparison of induction energies E_{ind} between the semi-empirical formulation based on Debye's formula and the theory calculated at the SAPT2/aug-cc-pVTZ level for the Ne-CH_3OH dimer. Vertical dashed lines indicate the equilibrium distance of the interacting dimer at different sites on the methanol molecule. The static linear polarizability of Ne-atom was set to $\alpha_0 = 0.392$ Å^3. Debye's formula for the permanent dipole-induced dipole interaction is given by $E_{ind} = E_{Debye}(R) = -\mu_{CH_3OH}{}^2 \alpha_{Gn} / (4\pi\varepsilon_0)^2 R^6$, with μ_{CH_3OH} standing for the dipole moment of methanol. The numeric coefficient is obtained when meV· Å^3 units are used.

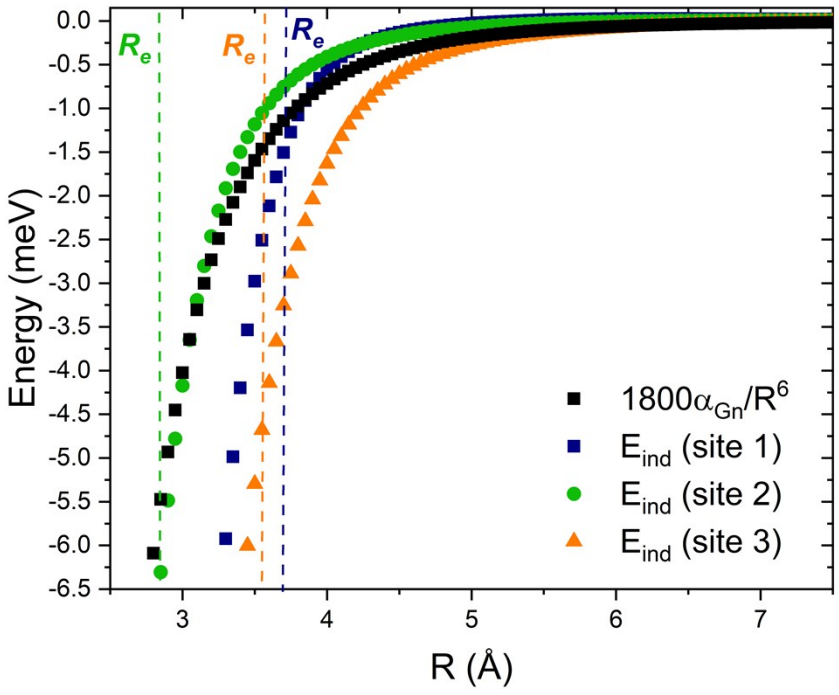

Figure S6. Comparison of induction energies E_{ind} between the semi-empirical formulation based on Debye's formula and the theory calculated at the SAPT2/aug-cc-pVDZ level for the Ar-CH_3OH dimer. Vertical dashed lines indicate the equilibrium distance of the interacting dimer at different sites on the methanol molecule. The static linear polarizability of Ar-atom was set to $\alpha_0 = 1.630\ \text{Å}^3$. Debye's formula for the permanent dipole-induced dipole interaction is given by $E_{ind} = E_{Debye}(R) = -\mu_{CH_3OH}{}^2 \alpha_{Gn} / (4\pi\varepsilon_0)^2 R^6$, with μ_{CH_3OH} standing for the dipole moment of methanol. The numeric coefficient is obtained when meV· Å³ units are used.

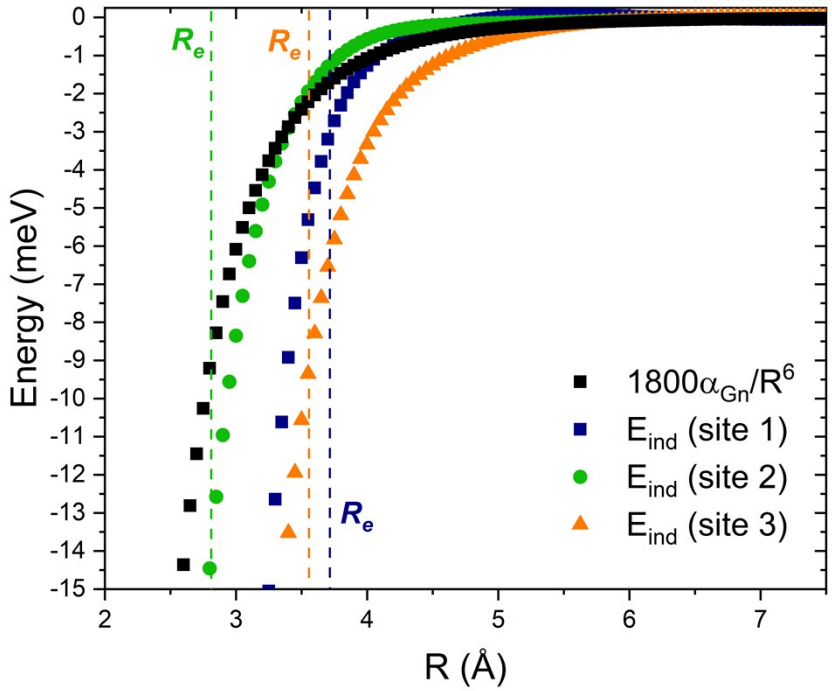

Figure S7. Comparison of induction energies E_{ind} between the semi-empirical formulation based on Debye's formula and the theory calculated at the SAPT2+(3)/aug-cc-pVTZ level for the Kr-CH_3OH dimer. Vertical dashed lines indicate the equilibrium distance of the interacting dimer at different sites on the methanol molecule. The static linear polarizability of Kr-atom was set to $\alpha_0 = 2.465\ \text{Å}^3$. Debye's formula for the permanent dipole-induced dipole interaction is given by $E_{ind} = E_{Debye}(R) = -\mu_{CH_3OH}{}^2 \alpha_{Gn} / (4\pi\varepsilon_0)^2 R^6$, with μ_{CH_3OH} standing for the dipole moment of methanol. The numeric coefficient is obtained when meV· Å³ units are used.

Table S6. Bound eigenvalues of the Nuclear Schrödinger Equation calculated with the potential energies of the interacting complexes Ng-CH_3OH for two rotational state $J = 0$ and 1.

Ng	Rotational State	Site 1	Site 2	Site 3
		$\varepsilon_{v,J}\ (cm^{-1})$		

He	$J=0$	$\varepsilon_{0.0}=12.17$	$\varepsilon_{0.0}=5.19$	$\varepsilon_{0.0}=14.00$
	$J=1$	$\varepsilon_{0.1}=11.47$	$\varepsilon_{0.1}=5.90$	$\varepsilon_{0.1}=13.27$
Ne	$J=0$	$\varepsilon_{0.0}=41.38$ $\varepsilon_{1.0}=19.55$ $\varepsilon_{2.0}=6.79$ $\varepsilon_{3.0}=1.24$	$\varepsilon_{0.0}=32.41$ $\varepsilon_{1.0}=13.57$ $\varepsilon_{2.1}=3.67$ $\varepsilon_{3.0}=0.38$	$\varepsilon_{0.0}=48.20$ $\varepsilon_{1.0}=24.84$ $\varepsilon_{2.0}=10.22$ $\varepsilon_{3.0}=2.74$
	$J=1$	$\varepsilon_{0.1}=41.15$ $\varepsilon_{1.1}=19.36$ $\varepsilon_{2.1}=6.64$ $\varepsilon_{3.1}=1.16$	$\varepsilon_{0.1}=32.04$ $\varepsilon_{1.1}=13.29$ $\varepsilon_{2.1}=3.48$	$\varepsilon_{0.1}=47.95$ $\varepsilon_{1.1}=24.63$ $\varepsilon_{2.1}=10.06$ $\varepsilon_{3.1}=2.63$
Ar	$J=0$	$\varepsilon_{0.0}=110.71$ $\varepsilon_{1.0}=79.69$ $\varepsilon_{2.0}=54.41$ $\varepsilon_{3.0}=34.71$ $\varepsilon_{4.0}=20.25$ $\varepsilon_{5.0}=10.43$ $\varepsilon_{6.0}=4.44$ $\varepsilon_{7.0}=1.35$ $\varepsilon_{8.0}=0.10$	$\varepsilon_{0.0}=94.70$ $\varepsilon_{1.0}=66.72$ $\varepsilon_{2.0}=44.24$ $\varepsilon_{3.0}=27.04$ $\varepsilon_{4.0}=14.80$ $\varepsilon_{5.0}=6.84$ $\varepsilon_{6.0}=2.54$ $\varepsilon_{7.0}=0.54$	$\varepsilon_{0.0}=131.95$ $\varepsilon_{1.0}=99.24$ $\varepsilon_{2.0}=71.81$ $\varepsilon_{3.0}=49.47$ $\varepsilon_{4.0}=31.97$ $\varepsilon_{5.0}=18.96$ $\varepsilon_{6.0}=9.98$ $\varepsilon_{7.0}=4.42$ $\varepsilon_{8.0}=1.40$ $\varepsilon_{9.0}=0.08$
	$J=1$	$\varepsilon_{0.1}=110.57$ $\varepsilon_{1.1}=79.56$ $\varepsilon_{2.1}=54.29$ $\varepsilon_{3.1}=34.60$ $\varepsilon_{4.1}=20.16$ $\varepsilon_{5.1}=10.35$ $\varepsilon_{6.1}=4.38$ $\varepsilon_{7.1}=1.31$ $\varepsilon_{8.1}=0.08$	$\varepsilon_{0.0}=94.47$ $\varepsilon_{1.0}=66.52$ $\varepsilon_{2.0}=44.06$ $\varepsilon_{3.0}=26.85$ $\varepsilon_{4.0}=14.53$ $\varepsilon_{5.0}=6.60$ $\varepsilon_{6.0}=2.30$ $\varepsilon_{7.0}=0.40$	$\varepsilon_{0.1}=131.80$ $\varepsilon_{1.1}=99.11$ $\varepsilon_{2.1}=71.68$ $\varepsilon_{3.1}=49.35$ $\varepsilon_{4.1}=31.87$ $\varepsilon_{5.1}=18.87$ $\varepsilon_{6.1}=9.91$ $\varepsilon_{7.1}=4.37$ $\varepsilon_{8.1}=1.36$ $\varepsilon_{9.1}=0.05$
Kr	$J=0$	$\varepsilon_{0.0}=133.26$ $\varepsilon_{1.0}=103.54$ $\varepsilon_{2.0}=78.00$ $\varepsilon_{3.0}=56.62$ $\varepsilon_{4.0}=39.30$ $\varepsilon_{5.0}=25.83$ $\varepsilon_{6.0}=15.82$ $\varepsilon_{7.0}=8.82$ $\varepsilon_{8.0}=4.32$ $\varepsilon_{9.0}=1.75$ $\varepsilon_{10.0}=0.42$	$\varepsilon_{0.0}=124.94$ $\varepsilon_{1.0}=96.67$ $\varepsilon_{2.0}=72.34$ $\varepsilon_{3.0}=51.94$ $\varepsilon_{4.0}=35.37$ $\varepsilon_{5.0}=22.48$ $\varepsilon_{6.0}=13.07$ $\varepsilon_{7.0}=6.82$ $\varepsilon_{8.0}=3.15$ $\varepsilon_{9.0}=1.13$	$\varepsilon_{0.0}=153.74$ $\varepsilon_{1.0}=123.00$ $\varepsilon_{2.0}=96.06$ $\varepsilon_{3.0}=72.90$ $\varepsilon_{4.0}=53.41$ $\varepsilon_{5.0}=37.50$ $\varepsilon_{6.0}=24.94$ $\varepsilon_{7.0}=15.51$ $\varepsilon_{8.0}=8.86$ $\varepsilon_{9.0}=4.52$ $\varepsilon_{10.0}=7.90$ $\varepsilon_{11.0}=0.43$
	$J=1$	$\varepsilon_{0.1}=133.17$ $\varepsilon_{1.1}=103.44$ $\varepsilon_{2.1}=77.44$ $\varepsilon_{3.1}=56.54$ $\varepsilon_{4.1}=39.23$ $\varepsilon_{5.1}=25.76$ $\varepsilon_{6.1}=15.77$ $\varepsilon_{7.1}=8.77$	$\varepsilon_{0.1}=124.82$ $\varepsilon_{1.1}=92.3247$ $\varepsilon_{2.1}=72.21$ $\varepsilon_{3.1}=51.82$ $\varepsilon_{4.1}=35.25$ $\varepsilon_{5.1}=22.38$ $\varepsilon_{6.1}=12.99$ $\varepsilon_{7.1}=6.76$	$\varepsilon_{0.1}=153.63$ $\varepsilon_{1.1}=122.90$ $\varepsilon_{2.1}=95.97$ $\varepsilon_{3.1}=72.81$ $\varepsilon_{4.1}=53.33$ $\varepsilon_{5.1}=37.42$ $\varepsilon_{6.1}=24.88$ $\varepsilon_{7.1}=15.45$

		$\varepsilon_{8.1} = 4.28$ $\varepsilon_{9.1} = 1.73$ $\varepsilon_{10.1} = 0.40$	$\varepsilon_{8.1} = 3.11$ $\varepsilon_{9.1} = 1.10$	$\varepsilon_{8.1} = 8.81$ $\varepsilon_{9.1} = 4.48$ $\varepsilon_{10.1} = 1.86$ $\varepsilon_{11.1} = 0.40$

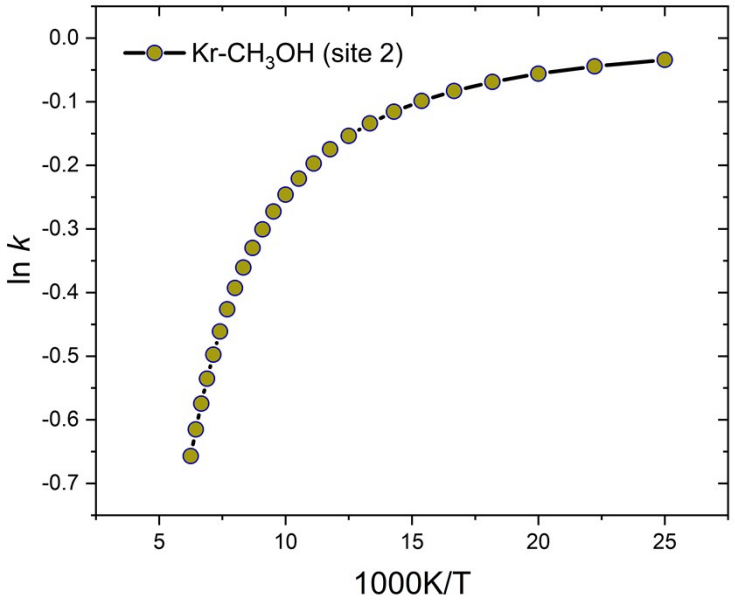

Figure S8. Equilibrium constant of complex formation of the Kr-CH_3OH van der Waals adduct as a function of temperature. For highly harmonic dimers the ln *k* vs *1/T* plot usually returns a Van't Hoff-like straight line, but for complexes in the present study, the significant contribution of the anharmonic constant $^{\omega_e x_e}$ induces a high distorted curve as the temperature increases and the complexes spend more time at large separation regions of the potential energy curve.